



# Dopaminergic Modulation of Local Non-oscillatory Activity and Global-Network Properties in Parkinson's Disease: An EEG Study

Juanli Zhang<sup>1,2\*</sup>, Arno Villringer<sup>1,3</sup> and Vadim V. Nikulin<sup>1,4\*</sup>

## OPEN ACCESS

### Edited by:

Aneta Kielar,  
University of Arizona, United States

### Reviewed by:

Eugenia Fatima Hesse Rizzi,  
Universidad de San Andrés, Argentina  
Shivakumar Viswanathan,  
Institute of Neuroscience  
and Medicine, Jülich Research  
Center, Helmholtz Association  
of German Research Centres (HZ),  
Germany

### \*Correspondence:

Juanli Zhang  
juanlizhang@cbs.mpg.de  
Vadim V. Nikulin  
nikulin@cbs.mpg.de

### Specialty section:

This article was submitted to  
Parkinson's Disease  
and Aging-related Movement  
Disorders,  
a section of the journal  
Frontiers in Aging Neuroscience

Received: 30 December 2021

Accepted: 31 March 2022

Published: 29 April 2022

### Citation:

Zhang J, Villringer A and  
Nikulin VV (2022) Dopaminergic  
Modulation of Local Non-oscillatory  
Activity and Global-Network  
Properties in Parkinson's Disease: An  
EEG Study.  
Front. Aging Neurosci. 14:846017.  
doi: 10.3389/fnagi.2022.846017

<sup>1</sup> Department of Neurology, Max Planck Institute for Human Cognitive and Brain Sciences, Leipzig, Germany, <sup>2</sup> Department of Neurology, Charité – Universitätsmedizin Berlin, Berlin, Germany, <sup>3</sup> Department of Cognitive Neurology, University Hospital Leipzig, Leipzig, Germany, <sup>4</sup> Neurophysics Group, Department of Neurology, Charité – Universitätsmedizin Berlin, Berlin, Germany

Dopaminergic medication for Parkinson's disease (PD) modulates neuronal oscillations and functional connectivity (FC) across the basal ganglia-thalamic-cortical circuit. However, the non-oscillatory component of the neuronal activity, potentially indicating a state of excitation/inhibition balance, has not yet been investigated and previous studies have shown inconsistent changes of cortico-cortical connectivity as a response to dopaminergic medication. To further elucidate changes of regional non-oscillatory component of the neuronal power spectra, FC, and to determine which aspects of network organization obtained with graph theory respond to dopaminergic medication, we analyzed a resting-state electroencephalography (EEG) dataset including 15 PD patients during OFF and ON medication conditions. We found that the spectral slope, typically used to quantify the broadband non-oscillatory component of power spectra, steepened particularly in the left central region in the ON compared to OFF condition. In addition, using lagged coherence as a FC measure, we found that the FC in the beta frequency range between centro-parietal and frontal regions was enhanced in the ON compared to the OFF condition. After applying graph theory analysis, we observed that at the lower level of topology the node degree was increased, particularly in the centro-parietal area. Yet, results showed no significant difference in global topological organization between the two conditions: either in global efficiency or clustering coefficient for measuring global and local integration, respectively. Interestingly, we found a close association between local/global spectral slope and functional network global efficiency in the OFF condition, suggesting a crucial role of local non-oscillatory dynamics in forming the functional global integration which characterizes PD. These results provide further evidence and a more complete picture for the engagement of multiple cortical regions at various levels in response to dopaminergic medication in PD.

**Keywords:** Parkinson's disease, dopaminergic medication, spectral slope, functional connectivity, graph theory

## INTRODUCTION

Parkinson's disease (PD) is the second most common neural degenerative disorder characterized by massive degeneration of dopaminergic neurons in the nigrostriatal dopamine system (Olanow et al., 2009). It has been increasingly recognized that PD is accompanied by functional disturbances both at subcortical and cortical levels (Braak et al., 2003; Boon et al., 2019). Clinically, dopamine loss is managed *via* dopaminergic therapy (DT). The dopaminergic system has been shown to have considerable and widespread modulatory influences on many brain structures including the cortex (Steiner and Kitai, 2001). While dopamine replacement therapy is efficient for improving the motor symptoms, the neural mechanisms of dopaminergic medication are not yet fully understood (Schapira, 2005).

In PD, it has been repeatedly reported that it is characterized by abnormal oscillatory synchrony in the basal ganglia-thalamus-cortical (BGTC) network in the beta frequency band (13–30 Hz) that could be modulated by dopaminergic medications and deep brain stimulation (DBS) (Brown, 2003; Wingeier et al., 2006; Kühn et al., 2009; De Hemptinne et al., 2015; Müller and Robinson, 2018). In the frequency domain, electrophysiological brain signals typically consist of a power-law  $1/f$  component and periodic oscillatory activities. While a majority of studies have so far been dedicated to the oscillatory activity, increasing evidence shows that non-oscillatory (aperiodic) activity also provides information about the intricate neuronal dynamics unfolding at different temporal scales (He et al., 2010; Voytek et al., 2015). A broadband aperiodic component of the spectrum is often represented by the slope of the fitted line in log-log space (known as spectral slope). The changes in spectral slope have been associated with neural development, healthy aging, and performance in working memory tasks (Voytek et al., 2015; Donoghue et al., 2020). In addition, previous studies have reported that it is altered in different pathologies, such as schizophrenia (Peterson et al., 2017; Molina et al., 2020) and ADHD (attention deficit/hyperactivity disorder) (Robertson et al., 2019). Importantly, it has also been demonstrated that the spectral slope is a potential indicator of the local excitation/inhibition balance (Gao et al., 2017; Colombo et al., 2019). In addition, TMS (transcranial magnetic stimulation) studies, which can directly probe the changes in excitation and inhibition, have shown that PD is accompanied by changes in cortical excitability (Ridding et al., 1995; Hanajima et al., 1996; Cantello, 2002). Thus, it would be important to test whether and how this measure is altered in PD, in particular with dopaminergic medication.

While regional changes could provide comprehensive understanding of the underlying local circuitry, the brain rather functions as a distributed network. Functional connectivity (FC) analysis allows us to understand how distinct regions interact, and graph-theory based approach enables a macroscopic perspective of brain connections on the regional and whole-brain network level. Many previous studies showed that network architecture is related to brain function or dysfunction (Bassett and Bullmore, 2009; Bullmore and Sporns, 2009). Using resting state fMRI (functional magnetic resonance imaging), it has

been intensively investigated how dopaminergic medication modulates brain FC in the BGTC network (Tahmasian et al., 2015). The most consistent finding across different rs-fMRI studies revealed decreased connectivity within the posterior putamen in PD (Tessitore et al., 2019), and that its cortical projections are modulated by dopaminergic medication (Herz et al., 2014). To date, few fMRI studies have adopted graph theoretical approach in PD, and the reported findings have been inconsistent. Specifically, compared to healthy controls, PD patients showed lower global efficiency (GE) (Sang et al., 2015), while no abnormalities in topographical property at the global level were observed in PD (Berman et al., 2016; Hou et al., 2018; Ruan et al., 2020). Both increase (Sang et al., 2015) and decrease (Hou et al., 2018) in nodal centrality have been observed in PD compared to healthy controls. In addition, it was found that levodopa administration significantly decreased local efficiency of the network (Berman et al., 2016), and conversely resulted in an increase in eigenvector centrality of cerebellum and brainstem in PD (Jech et al., 2013).

As for the EEG/MEG (electro- and magnetoencephalography) studies, compared to healthy controls, increased cortico-cortical FC in PD has been found primarily in alpha and beta frequency ranges, and cortico-cortical coherence was linked to the severity of the clinical symptoms (Silberstein et al., 2005; Stoffers et al., 2007, 2008; Bosboom et al., 2009; George et al., 2013; Miller et al., 2019). Dopaminergic medication induced changes in cortical synchronization have also been investigated by computing pairwise coherence across the entire montage using multi-channel EEG/MEG. However, both reduction of FC after dopamine medication (Silberstein et al., 2005; George et al., 2013; Heinrichs-Graham et al., 2014) and the absence of connectivity modulation were previously reported (Miller et al., 2019). Very recently, using advanced modeling analysis, in response to dopaminergic medication, increased cortico-cortical synchronization in beta band has been detected by taking into account the contribution from other sub-networks (Sharma et al., 2021). To capture the changes across the whole cortex, through the application of graph theoretical measures in EEG/MEG, previous studies have demonstrated abnormalities in topographical organizations of functional network in PD compared to healthy controls, suggesting that the interactions between cortical areas become abnormal and contribute to PD symptoms at various stages (Utianski et al., 2016). Furthermore, the alterations in network attributes were linked to both motor and cognitive dysfunctions (Olde Dubbelink et al., 2014; Boon et al., 2017). However, how the topological organization of the cortical functional network changes after dopaminergic administration remains rather elusive. To address this issue, we applied graph theory-based network analysis to investigate further changes in cortical connectivity in patients with PD after the administration of dopaminergic medication. Besides, previous studies have suggested a close link between the local excitation/inhibition balance and information transmission locally and globally (Deco et al., 2014), and the network's organizational structure (Zhou et al., 2021). Therefore, we asked whether and how the spectral slope, as a proxy of the local E/I ratio, would relate to the network-wise activity in the context of PD.

To further characterize the regional and functional network changes due to dopaminergic medication, we address the following questions. Regarding local properties: (1) How does the aperiodic property of the electrophysiological brain signal change in response to dopaminergic medication administration? With respect to cross-area interactions: (2) What is the effect of dopaminergic medication on functional connectivity? (3) Does dopaminergic medication induce alterations in the lower and/or higher level of the network architectures? (4) Do local changes in non-oscillatory component of neural activity influence functional network topology/organization? To answer these questions, we analyzed a publicly available dataset including EEG data of PD patients from ON and OFF dopaminergic medication conditions (George et al., 2013; Rockhill et al., 2020).

## MATERIALS AND METHODS

### Participants

The data analyzed in this study is open-source data (George et al., 2013; Swann et al., 2015; Jackson et al., 2019). This dataset includes resting state EEG data with a duration of around 3 min. Data were collected from 15 PD patients (8 female, average age =  $63.2 \pm 8.2$  years, mild to moderate disease with average disease duration of  $4.5 \pm 3.5$  years) during OFF and ON dopaminergic medication sessions. All participants were right-handed and provided written consent in accordance with the Institutional Review Board of the University of California, San Diego and the Declaration of Helsinki. For more information you may refer to George et al. (2013).

### Data Collection

EEG of patients with PD were recorded on two different days for ON and OFF medication sessions which were counterbalanced across subjects. For the OFF medication session, patients were requested to withdraw from their medication at least 12 h prior to the EEG recording. For the ON medication session, subjects took their medication as usual. A 32-channel EEG cap with BioSemi ActiveTwo system was used to acquire the EEG data with a sampling rate of 512 Hz. Two additional electrodes were placed over the left and right mastoids used for reference. During the EEG recording, participants were instructed to sit comfortably and fixate on a cross presented on the screen. Each recording session lasted at least 3 min. In addition, participants completed a few clinical assessments which were previously reported in George et al. (2013). In this study, we did not link the clinical scores of patients to the EEG measures as the authors of the original paper mentioned some uncertainty about these scores. Yet, to assure these two conditions represent two distinct parkinsonian states, we examined the change in the motor section of unified Parkinson's disease rating scale (UPDRS III) scores between the two conditions. Statistical analysis showed that there was a significant reduction of the clinical scores in ON condition (mean  $\pm$  SD:  $32.67 \pm 10.42$ ) compared to that in OFF condition (mean  $\pm$  SD:  $39.27 \pm 9.71$ ). Note, that in this dataset a healthy control group was also included. However, we focused on the comparison of data between ON and OFF conditions which is

also a standard study setup for differential parkinsonian states induced by medication in PD (Tinkhauser et al., 2017; Sharma et al., 2021).

### Data Pre-processing

EEG data were analyzed using EEGLAB (version 14.1.2; Delorme and Makeig, 2004) and FieldTrip toolboxes, together with customized scripts in Matlab (The MathWorks Inc., Natick, MA, United States). First, a high-pass filter at 1 Hz was applied to remove low frequency drifts (two-way FIR filter, order = 1,536, `eegfilt.m` from EEGLab). Subsequently, independent component analysis (ICA – infomax algorithm implemented in EEGLab) was used to remove artifactual sources of cardiographic components, eye movements and blinks, and muscle activity in the data. Further, channels with inadequate quality were rejected by visually inspecting whether their spectra demonstrated residual EMG at higher frequency ranges [on average  $5.4 \pm 3.1$  for OFF and  $5.2 \pm 2.8$  for ON, no difference between conditions ( $p = 0.6606$ )]. Bad channels were interpolated with neighboring electrodes using a method of spherical splines (EEGLab function “`eeg_interp`”). Next, data were examined visually for the presence of residual artifacts and segments contaminated by gross artifacts and these events were marked and then excluded from further analysis [on average  $172.5 \pm 22.7$  s in OFF and  $165.5 \pm 33.6$  s in the ON condition remained, no difference in the number of rejected data points ( $p = 0.3591$ )]. Subsequently, data were re-referenced to the common average.

## DATA ANALYSIS

### Power Spectral Density

Power spectral density (PSD) was calculated using the function “`pwelch`” in MATLAB, with a Hamming window of 512 samples (i.e., 1 s) and a 50% overlap. Beta band power was estimated as the averaged PSD in the beta frequency range (13–30 Hz). In addition, in line with a previous study (Donoghue et al., 2020), we utilized another way of estimating the oscillatory beta power by accounting for the overall spectral slope. For this purpose, we subtracted the spectral slope (measured by a fitted line in a log-log space) and estimated the beta power on the residuals of the PSD.

### Power Spectral Density Slope

To reduce contamination from high frequency non-neuronal noise, we estimated the slope of the PSD in a frequency range of 2–45 Hz. A three-step robust regression method was used to estimate the slope based on the computed PSD. This method was proposed and applied by Colombo et al. (2019). First, a least-squares linear line was fitted to the raw PSD using the function “`robustfit`” in MATLAB in the log frequency-log PSD space. Second, frequency points with larger than 1 median absolute deviations of the PSD residuals were identified as oscillatory peaks. Continuous frequency bins surrounding these peak frequencies were considered as the base of the oscillatory peaks and were also excluded for the further step. Last, a second least-squares fit was performed on the rest of the frequency ranges. We took the slope (with the sign) of the second fitted

line as the final spectral slope of the PSD. Thus, a more negative slope demonstrates a steeper decay, while a less negative slope represents a flatter one. One advantage of this method is that it considers the potential bias resulting from linearly spaced frequency bins being estimated with a logarithmic scale. Therefore, before the regression procedure, the PSD curve was up-sampled with logarithmically distributed frequency bins. For more details, please refer to the study by Colombo et al. (2019).

## Functional Network Analysis

A network is constructed by a collection of nodes and links between pairs of nodes. In this study, we defined each node as a brain region approximately represented by each channel, while links represent the connectivity between pairs of channels. FC between the brain areas was determined by computing the lagged coherence which accounts for the volume conduction issue. Each network can be represented by a symmetrical  $32 \times 32$  adjacency matrix.

### Functional Connectivity

Functional connectivity measure was quantified by the lagged coherence between all the channel pairs in a frequency range of 1–35 Hz with resolution of 1 Hz. This metric quantifies the strength of phase coupling between two signals by eliminating the effects of volume conduction (Pascual-Marqui, 2007; Pascual-Marqui et al., 2011), and it has been shown to be even more suitable than phase lag index for the application of connectivity estimation when using EEG and MEG (Hindriks, 2021). Its value ranges between [0, 1]: “0” stands for no coupling, and “1” represents perfect coupling. This measure has been utilized in earlier EEG studies (Milz et al., 2014; Vecchio et al., 2021). FC in an oscillatory frequency band was acquired by averaging the FC values over the respective frequency range (for instance beta band FC was obtained by averaging the FC values over 13–30 and 8–12 Hz for the alpha band). To investigate whether medication could result in changes in FC in oscillatory frequency band across the whole brain (neighboring areas and remote regions), we applied a seed-based connectivity comparison approach. This means that the connectivity was calculated between a given electrode (seed) and all other electrodes for each subject. Then, whole-head connectivity was compared between conditions using a cluster-based permutation test to account for multiple comparisons.

### Network Measure

We estimated the brain network metrics based on the scalp sensor-based EEG connectivity matrix. Although often performed in source space, due to a small number of channels (Lantz et al., 2003) we did it rather in sensor space similar to previous studies (Stam et al., 2007; Zeng et al., 2015; Chai et al., 2019; Sun et al., 2019; Mitsis et al., 2020; Smith et al., 2021). In the discussion, we mention and discuss limitations associated with the estimation of graph metrics in sensor space.

#### Node Degree

Node degree estimates the number of edges connected to each node. To estimate the importance of each node (each

channel in our case), node degree centrality weighted by edge importance (the connection is stronger, edge weights are larger) was utilized for this purpose. Specifically, we used the function “Centrality” implemented in Matlab for this measure (parameter “importance” specified by edge weights).

### Graph Theory Based Complex Network Measures

**Overall Functional Connectivity.** For each individual FC matrix, the overall FC was obtained by averaging all the connectivity values across all the pairs of the connection in a matrix.

**Proportional Thresholding.** Proportional thresholding is a commonly applied approach to remove connections with lower strength and to obtain a sparse connectivity matrix for computing the network properties based on graph theory. Here, we applied a proportional threshold to keep a consistent density of the connections across individuals (Bassett and Bullmore, 2009; van den Heuvel et al., 2017). If a proportional threshold (PT%) is applied to a functional network, all the strongest PT% of the connections are preserved and set to 1; the other connections are set to 0. As suggested by Rubinov and Sporns (2010), networks should be ideally characterized and show consistent patterns across a broad range of thresholds. These threshold values are often determined differently across studies. Therefore, in this study we examined a wide range of thresholds ranging from 36 to 4% (resulting in networks with around 20–200 links) in steps of 2%, similar to a previous study (van den Heuvel et al., 2017). To show how the network looks like, in **Figure 1**, we plotted the grand mean networks within each group at differential thresholding values (20, 10, and 2%).

**Graph Metrics.** Various measures characterize a network's structure. Two fundamental ones are included here: clustering coefficient (CC) and global efficiency (GE). These two basic graph metrics were computed as implemented in the Brain Connectivity Toolbox (Rubinov and Sporns, 2010). Clustering coefficient is a commonly used measure to quantify the functional network segregation. It is defined as the fraction of triangles (ratio of the present and total possible number of connected triangles) around an individual node and is equivalent to the fraction of a node's neighbors that are neighbors of each other (Watts and Strogatz, 1998). The clustering coefficient of a network CC is the average clustering coefficient across all the nodes in the network. It reflects the prevalence of clustered connectivity around individual nodes (Rubinov and Sporns, 2010): the larger the CC, the greater the degree of functional segregation.

The other metric, GE, was used to quantify the functional network integration. This is based on a basis measure – shortest characteristic path length. Paths are sequences of distinct nodes and links, with shortest paths between two nodes defined as the path with the fewest edges in a network (the sum of the number of its constituent edges is minimized). GE for a network, obtained by the average inverse shortest path length between all the pairs, is a measure of functional network integration: the larger the GE, the greater the degree of global integration. All these measures

were computed with an open source Matlab toolbox (Rubinov and Sporns, 2010).<sup>1</sup>

## Statistical Tests

Non-parametric Wilcoxon signed rank test was performed for the comparisons of measures in PD OFF and ON states. Spearman's correlation coefficients were calculated to estimate the relations between different measures. We applied the false discovery rate (FDR) procedure (Benjamini and Hochberg, 1995) to correct for multiple tests (correlation calculation) across channels. Significance is reported when FDR-corrected  $p$ -values are below 0.05.

To account for multiple comparisons of metrics across all channels, we performed a channel space cluster-based permutation test using the "Monte Carlo" method, as implemented in FieldTrip (Oostenveld et al., 2011). At sample level (each channel in this case), a dependent  $t$ -test was utilized to estimate the effect. A total of 1,000 randomizations were performed across groups (ON and OFF conditions) and for each permutation. Additionally, the single sample  $t$ -values are thresholded at the 95th quantile, and cluster-level statistics (sum of  $t$ -values within each cluster) were computed and the largest cluster statistic was taken to build a null distribution. We then compared the observed cluster-level statistic from the empirical data against the null distribution derived from the permutation procedure.  $p$ -Values below 0.05 (two-tailed) were considered significant. A positive or negative cluster demonstrates a significant difference between two conditions (OFF > ON) or (OFF < ON).

## RESULTS

### Spatial Specificity and Effects of Medication on Spectral Slope

The grand mean of PSD averaged from all channels across subjects in each group is shown in **Figure 2A**. One can observe that the PSD decay in PD OFF was shallower compared to the PSD decay in PD in the ON condition. The spectral slope was computed for each channel and each subject. **Figure 2B** shows the topography of the grand mean of the spectral slope across all subjects within each group (upper panel for OFF and lower panel for ON condition). As shown in **Figure 2B**, for both groups, spectral slopes were more negative (steeper slopes) along the fronto-central-parietal midline of the brain and flatter in the other regions. In general, the ON condition was characterized by a more negative slope than that in the OFF condition.

We investigated the difference between the two conditions for all channels. As described in section "Materials and Methods," we applied a non-parametric cluster-based permutation test to correct for multiple comparisons in the channel space. When comparing slope values in PD OFF with those of PD ON, a significant positive cluster ( $p = 0.0220$ ) indicated an increased slope (flatter) in PD OFF. This difference

demonstrated a lateralized pattern covering mostly left central region (**Figure 2C**).

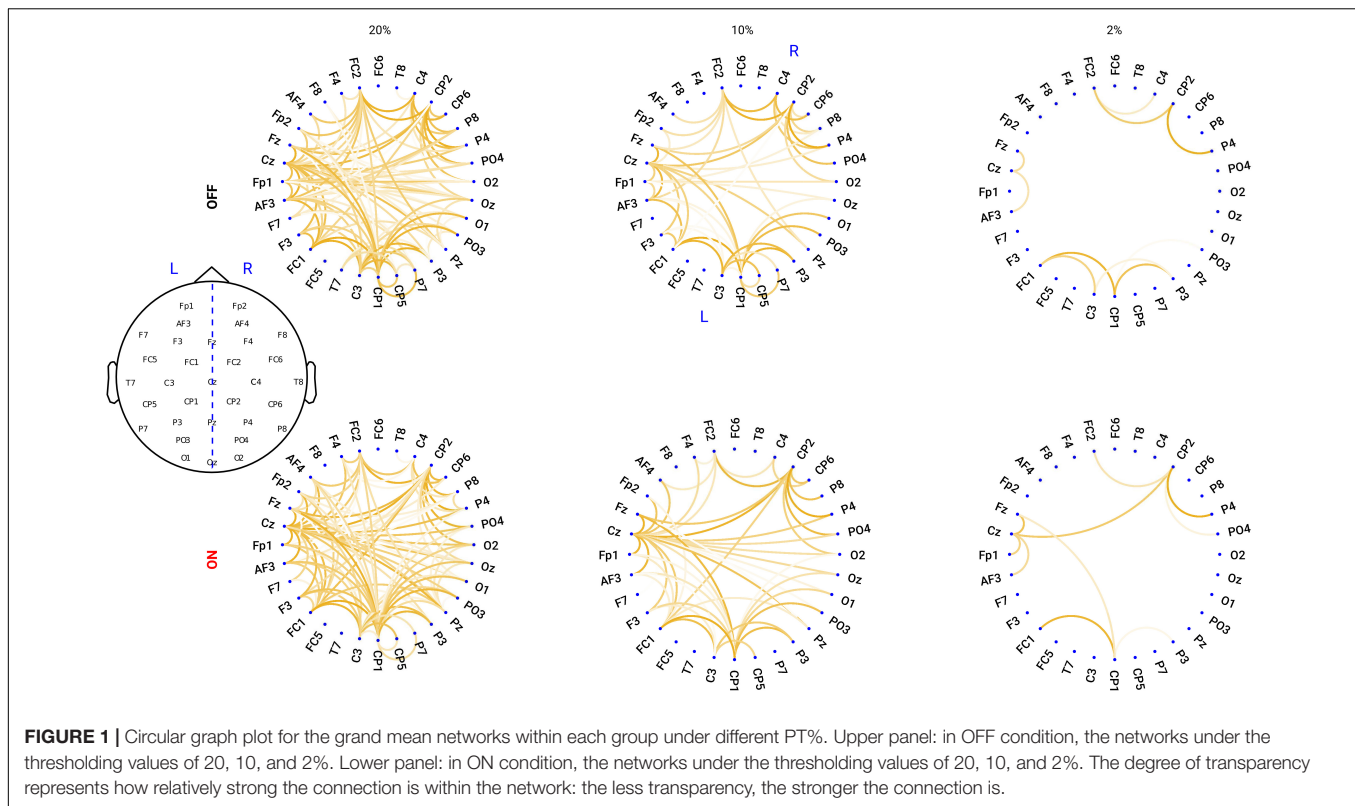
### No Beta Power Difference Between Conditions Before and After Correcting for the Slope Effect

Previous studies have demonstrated inconsistent changes in cortical beta power: an increase of beta power after dopaminergic medication (Melgari et al., 2014) and insignificant cortical beta power changes after DT in PD (George et al., 2013; Miller et al., 2019). Since we showed that the background slope was significantly modulated by dopaminergic medication (significantly steepened by the medication), we assumed that insignificant beta power reports might partly be attributed to the overall broadband slope changes. To test this assumption, we first applied a traditional approach to estimate the beta band power on the raw PSD. We computed the mean PSD value in the beta frequency range (13–30 Hz) for each channel and each subject in each group. Cluster-based permutation tests in channel space showed no significant difference in beta power between conditions (**Figure 3A**). Next, to address whether this finding might be due to a flattened background spectral slope (as observed in the PD OFF vs. ON comparison) on the top of which oscillations were present, we used a second approach controlling for the spectral slope to estimate beta-oscillation power for each channel and subject. **Figure 3B** shows the grand mean of the residuals of the PSD across all channels after accounting for spectral slope. By averaging the PSD values in the same frequency range of 13–30 Hz, beta band power for each channel and each subject was re-calculated. Cluster-based permutation tests identified two non-significant negative clusters (OFF-ON) ( $p = 0.0739, 0.0939$ ), mainly localized in bilateral centro-parietal regions (CP5, CP1 and C4, CP6, **Figure 3C**). This demonstrates that even after accounting for the background slope effect, there were no significant beta power changes between the two medication conditions.

### Functional Connectivity in Beta Band Is Increased After Medication

First, we predominantly focused on the sensorimotor seed-based connectivity changes, which typically include C3 and C4 electrodes (Swann et al., 2015; Miller et al., 2019). The upper panel of **Figure 4A** depicts the FC between C3 and one of the representative channels from the parietal region (Pz) along a wide frequency range (1–35 Hz). One can observe clear peaks around the alpha and beta frequency bands for both the ON and OFF conditions. Next, we averaged the connectivity values in the beta frequency range (13–30 Hz) as a measure of beta band FC. As described above, C3 seed-based beta band connectivity was compared between medication conditions. A negative cluster localized in the parieto-occipital region (OFF < ON,  $p = 0.007$ ) was identified as shown in the upper panel of **Figure 4B**, demonstrating a lower connectivity between C3 and parieto-occipital regions in the OFF compared to the ON conditions. However, there was no significant difference in the comparison of C4 seed-based connectivity between conditions.

<sup>1</sup><http://www.brain-connectivity-toolbox.net>

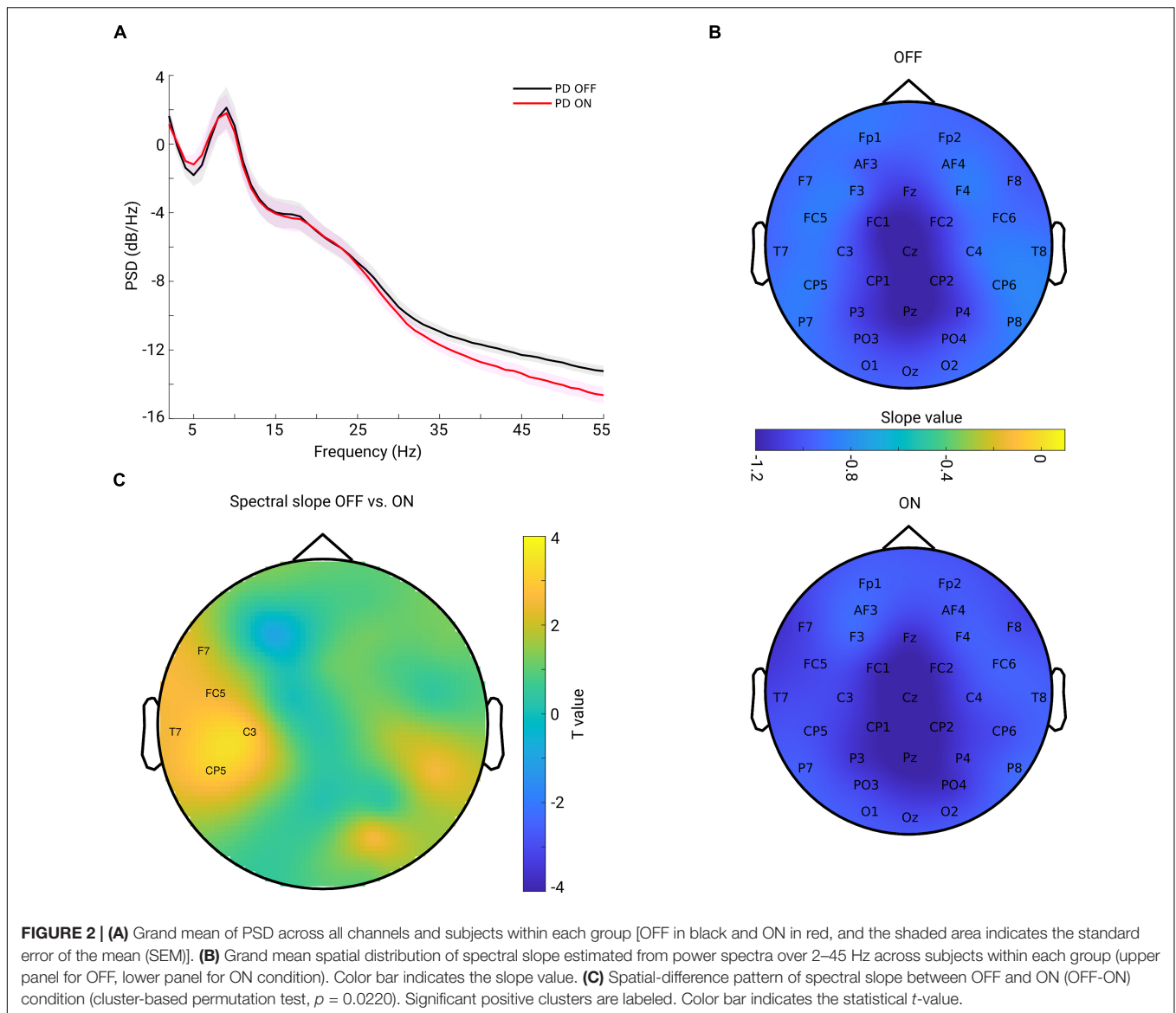


Furthermore, to investigate whether the frontal region showed altered synchronization with other regions, we chose one of the representative channels in the frontal area [Fz, which is typically within the cluster of electrodes near the supplementary motor area (Casarotto et al., 2019)] and performed the same analysis as for electrode C3. As shown in the lower panel of **Figure 4A**, there were obvious peaks in the broad oscillatory frequency range (alpha and beta) for both conditions. The lower panel of **Figure 4B** shows the topographical pattern for the comparison between OFF and ON conditions, and a significant negative cluster ( $p = 0.0250$ ) localized primarily in the parietal region. This demonstrated that the synchronization between Fz and parietal regions in the beta band was significantly enhanced in the ON compared to OFF condition in PD. Finally, we performed the same analysis for the other channels to demonstrate whole-head comparisons in a head-in-head plot (**Figure 4C**). As in C3 and Fz seed-based connectivity comparisons, the other channels in seed-based connectivity also showed significant increase in ON compared to OFF conditions. Significant clusters ( $p < 0.05$ ) are marked by warm color. In general, the topographies showed significant alterations in synchronization between frontal, central, and parieto-occipital regions. To show that these connectivity effects are not mainly driven by the power of the beta oscillation itself, we also examined the PSD and connectivity profiles and found that in the beta band the peaks of the connectivity between the two channels do not coincide with the peaks of the power from either of the relevant channels (see **Supplementary Figure 1**). Therefore, we conclude that the connectivity effect estimated from the

lagged coherence is not driven by the power and rather reflects phase-driven interaction. In addition, due to presence of peaks of the FC in the alpha band, we used the same approach to explore the FC changes in alpha band (8–12 Hz). Yet, there was no significant cluster detected for all the possible seeds when comparing the two conditions. Due to our predominant interest in the beta frequency range and pronounced effects observed in this frequency band, in the rest of the study we focus on the measures from the beta band.

## Node Degree in Centro-Parietal Region in Beta Band Is Increased After Medication

Next, we tested whether the local level of a network feature, namely the node degree, was modulated by the medication effect. For this purpose, we calculated the node degree (from the connectivity in the beta band) for each channel and each subject. **Figure 5A** shows the topographical maps of the grand mean of the node degree across subjects within each group. As can be seen from **Figure 5A**, both groups showed a spatial specificity regarding the degree distribution (left for OFF and right for ON conditions): a higher level of the node degree in central areas than in other regions. This demonstrates that the central region might, in general, interact more with other regions in the whole brain network. Next, we compared the node degree between conditions for all channels using a cluster-based permutation test. **Figure 5B** shows the spatial difference pattern – a significant negative cluster was detected ( $p = 0.0140$ , OFF vs. ON, shown by labels)

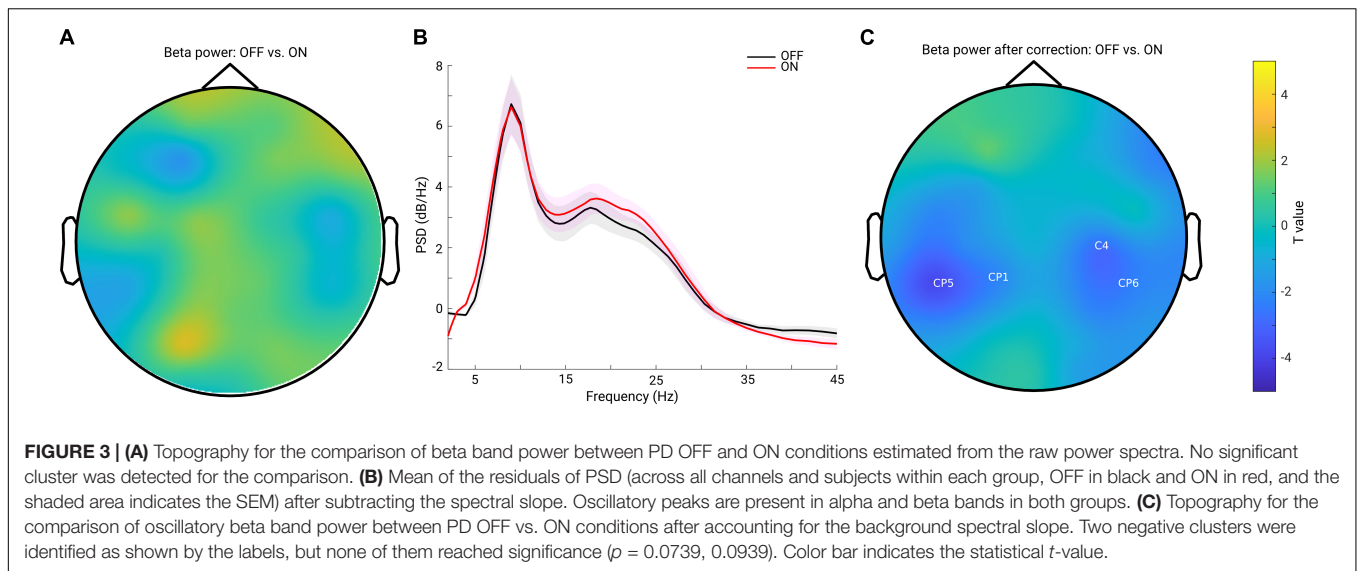


mainly in the centro-parietal region, suggesting that medication modulated the node degree of the beta band functional network in a way that the connectivity of the centro-parietal region became more pronounced in the whole network. Thus, this analysis further confirmed our findings obtained from seed-based connectivity analyses, revealing that synchronization was up-regulated by medication specifically between the centro-parietal region and other regions.

### No Significant Change in the Global Network Topology: Either in Network Segregation or Network Integration Measure

To answer the question whether the global network structure is modulated by medication, we estimated the two fundamental features of a network: the GE for measuring functional network

integration and the CC for measuring network functional segregation. We report the comparison results for both of the measures across a wide range of proportional thresholding values (36–4%, with a step of 2%) between the two conditions. Since it has been shown that differences in overall FC could have predictable consequences for between-group differences in network topology (van den Heuvel et al., 2017), we here first checked whether in our data there could be a possible bias for the comparison. However, no significant difference in overall FC between condition comparisons was found (Wilcoxon signed rank test, two-tailed,  $p = 0.1514$ ). Thus, the overall FC is probably not a significant bias in the comparisons we performed as shown below. As seen in **Figure 6A**, across the whole range of thresholding (36–4%), the mean GE across subjects in the OFF condition (in black) almost overlapped with that from the ON condition (in red). As for clustering coefficient, the grand mean of CC in the OFF condition (black line) showed higher values



than those in the ON condition (red line) across all thresholding values (**Figure 6B**). However, the statistical comparison did not indicate a significant difference in GE ( $p > 0.05$ ,  $p$ -values shown in dashed orange line, right  $y$ -axis), or in CC between the two conditions ( $p > 0.05$ ,  $p$ -values shown in dashed orange line, right  $y$ -axis). Thus, controlling for the overall FC values and across a wide range of thresholding values, we were not able to demonstrate a significant impact of medication on global network configuration.

### Spectral Slope (Local and Global) Predicts the Network Global Efficiency in OFF Medication

Next, we asked how the spectral slope, as a proxy of measuring local E/I balance, would relate to the brain functional network; thus, we investigated a possible relationship between spectral slope and network topology. First, we averaged the spectral slope across all channels to represent an overall slope (referred to as global slope) for each subject. Spearman's correlation was performed between global slope and network metrics (GE and CC) derived under an exemplary thresholding value at 20% in both groups. As shown in the scatter plot in **Figure 7A**, GE negatively correlated with global slope ( $Rho = -0.7643$ ,  $p < 0.001$ ) in the OFF condition. In contrast, no such association was observed in the ON condition ( $Rho = -0.1036$ ,  $p = 0.7144$ ). Next, we performed a correlation analysis for the channel-wise slope (referred to as local slope) and network GE in the OFF condition. This analysis revealed a significant negative relationship between local slope values and network GE as shown in the topographical map (channels demonstrating significance are highlighted by label, FDR-corrected) in **Figure 7B**, and this relationship was most pronounced in the left centro-parietal area. There was no significant relationship between local slopes and GE in the ON condition. In addition, we examined if the relationship we observed at the 20% thresholding could be obtained regardless of the specific thresholding value. We performed the correlation

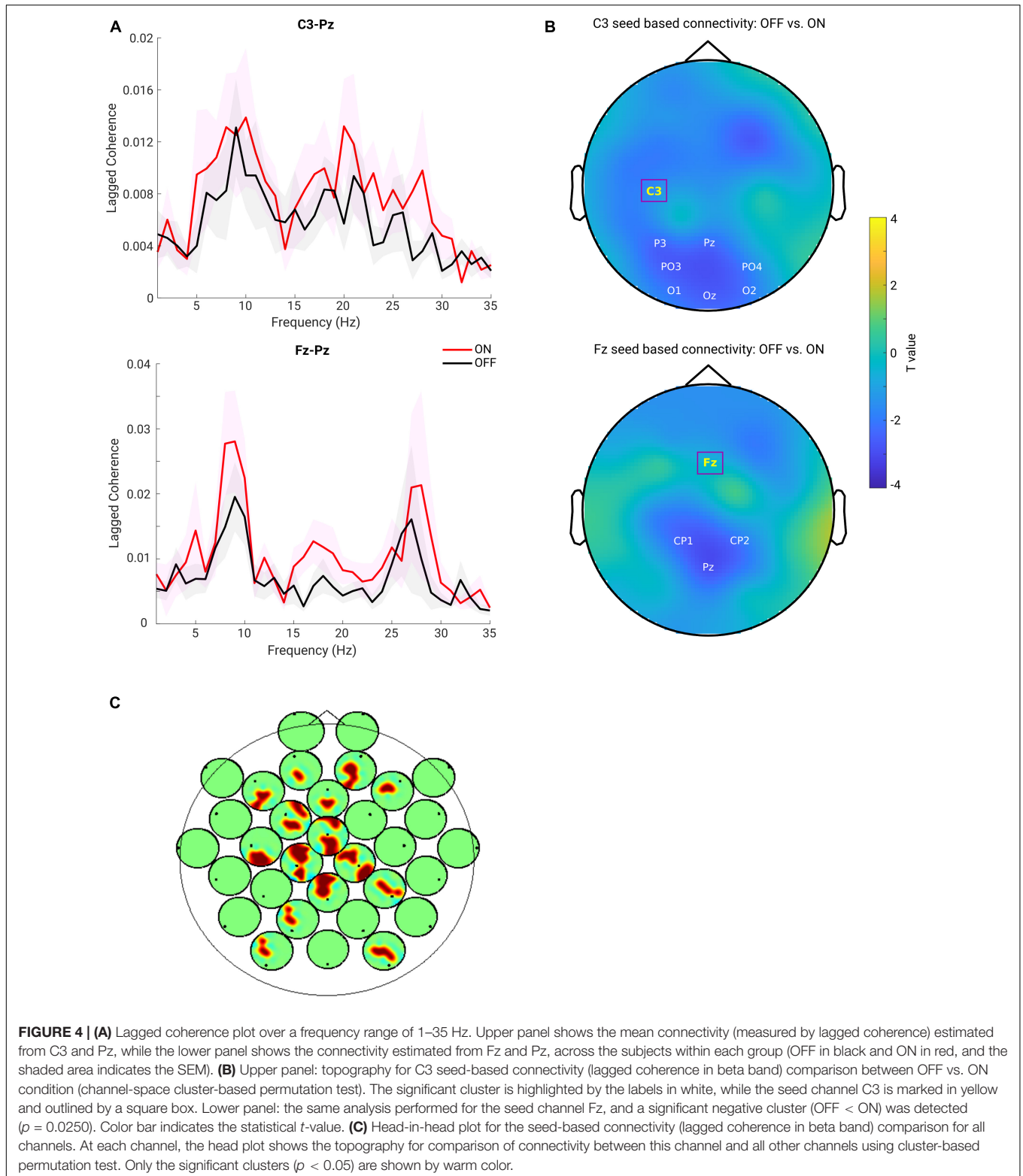
analyses between global slope and network GE across the whole range of thresholding values (36–4% with a step of 2%) in the OFF group. As shown in **Figure 7C**, almost across all PT%, the negative association between global slope and network GE was present consistently ( $p < 0.05$ ,  $p$ -values shown in dashed orange line, right  $y$ -axis), except under an extreme thresholding value of 4%. The spatial correlation pattern between local slope and network GE was also examined under the same range of thresholding values, and consistently negative relations between local slope from the centro-parietal region and network GE were observed (see **Supplementary Figure 4**). These results showed that global slope negatively correlated with network GE across a wide range of thresholding values, and a further topographical correlation map between local slope and network GE demonstrated a region-specific pattern.

### Control for the Discontinuity in the Data

To assure that the estimation of the metrics is not affected by signal discontinuity introduced by removing the artifacts, we additionally performed the main analyses respecting the cutting borders. Consistently, we obtained very similar results with respect to spectral slope and lagged coherence. The differences between the two medication conditions remained unchanged. A detailed report can be found in **Supplementary Figures 2, 3**.

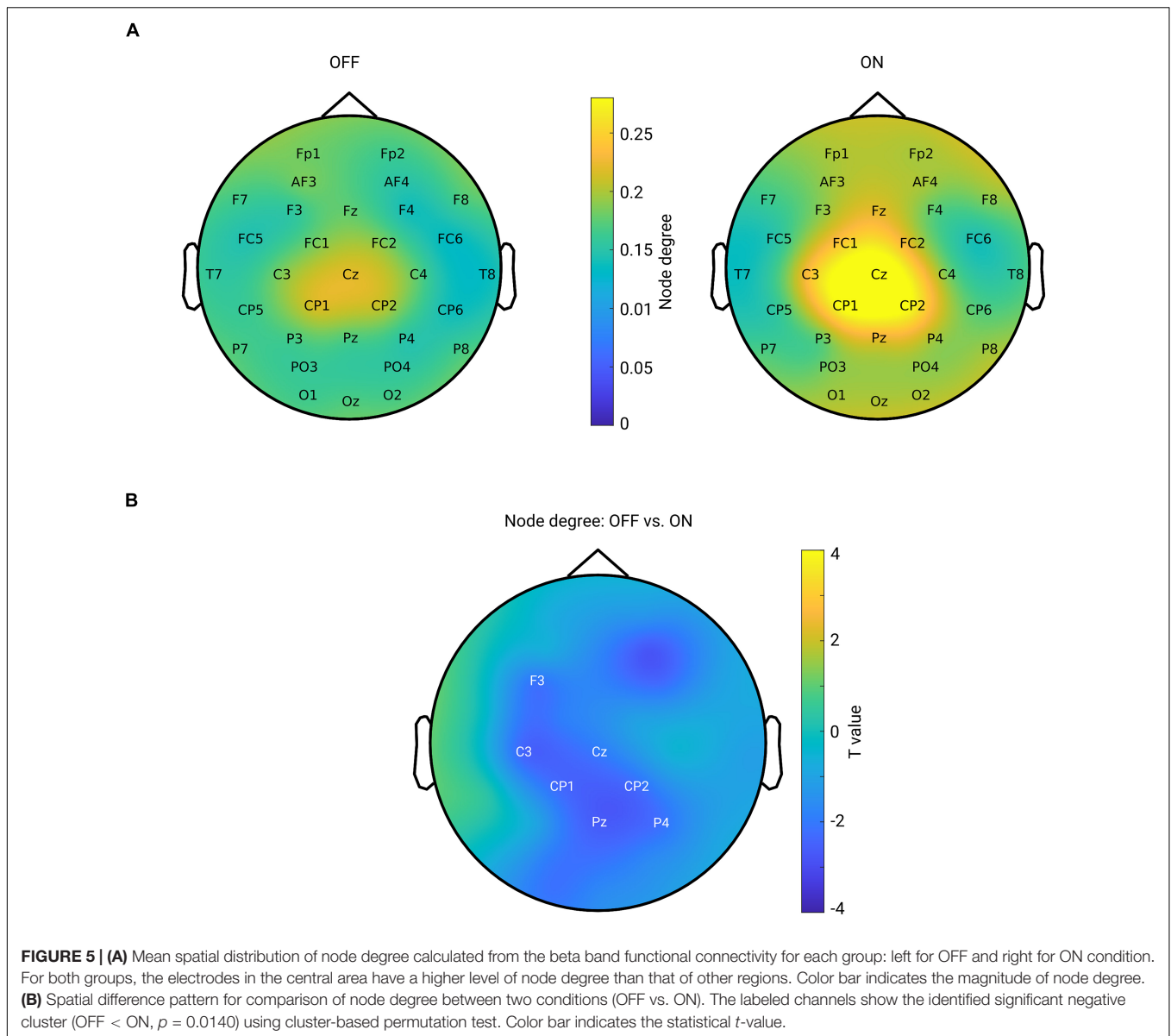
## DISCUSSION

In this study, we investigated local and global changes induced by dopaminergic medication in a cohort of PD patients using non-oscillatory spectral slope measure and connectivity analysis in resting state EEG. Locally, we estimated the slope of the non-oscillatory wideband background activity and showed that the left central region had a significantly decreased (steeper) spectral slope during the ON compared to OFF medication state. In addition, in ON compared to OFF, we observed an increase in the FC in the beta band, mainly between centro-parietal and



frontal regions. Further, graph theory-based analysis showed an enhanced node centrality in particular in the centro-parietal regions but no significant alteration in the complex level of network topology (GE or CC). Lastly, we found a strong negative

relationship between spectral slope (locally and globally) and network's GE in the OFF condition, where a flatter slope was associated with a smaller degree of GE of the functional network. These findings provide further evidence for the engagement of

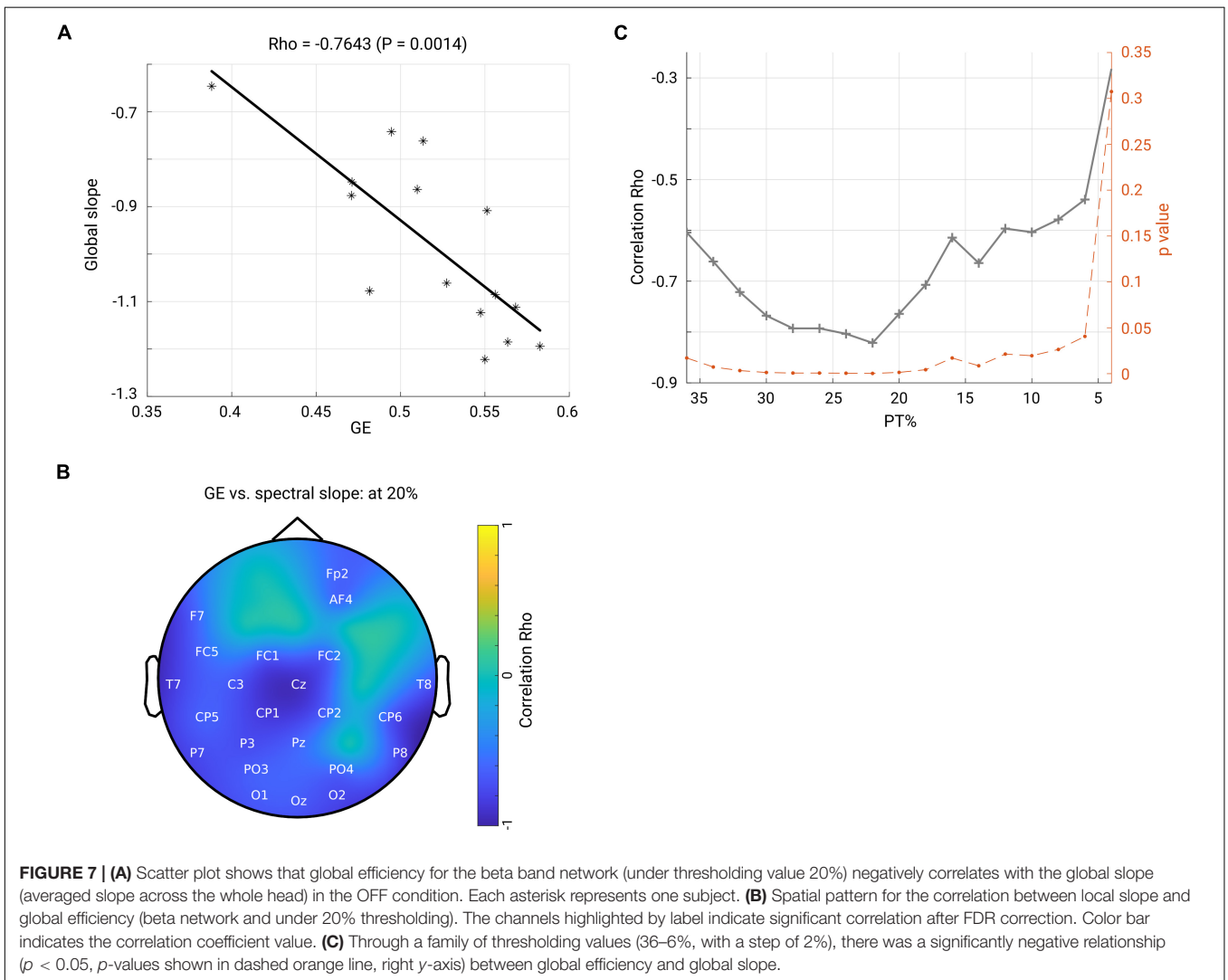
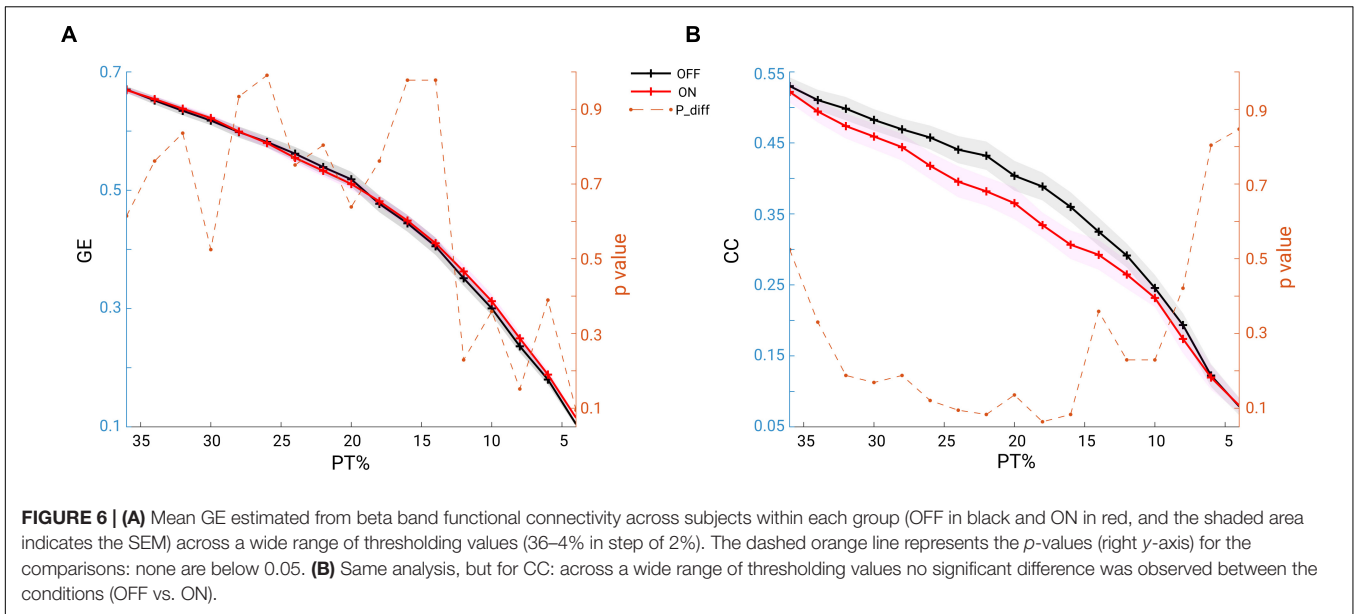


multiple cortical regions in response to dopaminergic medication in PD, which in turn may indicate that the therapeutic efficacy of dopaminergic medication may relate to both regional and global changes in cortical activity.

## Non-oscillatory Background Spectral Slope

Using multi-channel resting state EEG, we observed that patients with PD in the medication OFF condition had an increased (flatter) spectral slope compared to medication ON condition. This effect was found to be spatially specific to the left central region. The spectral slope, a metric to quantify this background power spectrum, has been reported to be altered in the first year of development, healthy aging and in mental disorder such as schizophrenia (Peterson et al., 2017; Donoghue et al., 2020;

Molina et al., 2020; Schaworonkow and Voytek, 2021), and could also predict the dynamic behavioral outcome in working memory tasks (Voytek et al., 2015; Donoghue et al., 2020). In our study, we observed that the spectral slope steepened in ON compared to OFF conditions. Given that previous studies demonstrated that healthy aging is accompanied by flattening of the spectral slope (Voytek et al., 2015; Cesnaite et al., 2021) and that neural electrophysiological biomarkers associated with PD are already present in the apparently healthy aging brain (Zhang et al., 2021), one can speculate that PD might be accompanied by a flattening of the power spectra and that dopaminergic medication might reverse this flattening effect. The effect was found most pronounced in the left central area (strongest at C3 electrode in the detected cluster), which might indicate a modification over the sensorimotor area by the medication. The broadband spectral slope underlying the dopamine medication modulation effect



in patients with PD may thus potentially serve as a biomarker sensitive to dopamine replacement therapy. At the same time, even though we carefully cleaned the data and removed artifacts which might contribute to the estimation of spectral slope, we could not completely rule out this confounder. However, we would like to emphasize that this is unlikely to drive the effect of spectral slope we observed, otherwise one would expect a spatial pattern which shows strongest difference over the frontal or temporal areas (which cover large muscle groups and prone to be contaminated by the muscle activity). Additionally, as we mentioned before, the spectral slope has been shown to index the E/I balance, and we will discuss the implication of this finding below (see section “Spectral Slope and Network Global Efficiency: Local E/I Balance and Global Network”).

### Power of Beta Oscillation

Previous studies have demonstrated an increase in cortical beta-band power in PD compared to healthy controls and alleviated beta band synchrony after medication administration (Stanzione et al., 1996) and attenuation by DBS (Whitmer et al., 2012). On the other hand, other studies have also reported an opposite effect—an increase of beta band power after dopaminergic medication (Melgari et al., 2014). In addition, some studies demonstrated that dopaminergic medication did not have any effect on cortical beta power (Stoffers et al., 2007; George et al., 2013; Swann et al., 2015; Miller et al., 2019). Importantly, all previous PD studies on this topic have only considered total power of beta without separating it into oscillatory and 1/f aperiodic components. In the present study, we tested the impact of the removal of the aperiodic part of the spectrum on the estimation of oscillatory power. We found that a conventional approach to estimate oscillatory power based on the raw PSD resulted in a non-significant difference in beta band in the PD OFF compared to ON state. After accounting for the spectral slope changes, a marginal increase of beta power was detected in the centro-parietal regions in the comparison between the ON and OFF conditions, yet this difference failed to reach significance. Our data thus suggests that even though the beta-band power estimation by the conventional approach might be partly affected by the background wideband PSD spectra, correcting the effect still does not yield a clear and statistically significant difference between the ON and OFF conditions. Thus, in line with some previous studies (George et al., 2013; Swann et al., 2015; Miller et al., 2019), we further confirm that with and without considering the background slope effect, there was no difference in beta power between the medication conditions. In addition, we discuss a possible relation of our findings to prior studies which were based on the same dataset. The only intersecting aspect across all these prior studies and ours is the investigation of beta-band power change during resting state. Consistently with what have been reported by George et al. (2013) and Swann et al. (2015), our study demonstrated there was no beta power change between the two medication states. Importantly, in our study, we have examined a possible bias from the overall PSD slope effect and showed that even when considering it there was no spectral power change in beta frequency range between the two conditions. Yet, we suggest

that future studies should take into account the effect of the aperiodic spectral component for the comprehensive evaluation of oscillatory power changes in PD.

### Functional Connectivity

We observed a significant increase in FC of beta oscillations in the ON compared to OFF condition, in particular between the centro-parietal regions with frontal regions. Previous studies have demonstrated a presence of beta-band coherence between STN (subthalamic nucleus) and multiple cortical regions, including sensorimotor (Hirschmann et al., 2011, 2013; Litvak et al., 2011), parietal and frontal areas (Litvak et al., 2011) in the OFF medication condition in patients with PD. Dopaminergic medication can also alter the beta-band connectivity between STN and cortical regions (Stoffers et al., 2008; Litvak et al., 2011; Hirschmann et al., 2013; van Wijk et al., 2016). As for the cortico-cortical connectivity, dopaminergic medication administration was shown to either reduce interactions between cortical areas (Silberstein et al., 2005; George et al., 2013; Pollok et al., 2013; Heinrichs-Graham et al., 2014) or not to produce any significant changes (Miller et al., 2019). In a very recent study using combined STN-LFP (local field potential) and MEG recordings, the authors discovered differential effects of dopaminergic medication in different levels of networks (Sharma et al., 2021). Specifically, in the cortico-cortical network, sensorimotor-cortical connectivity across multiple regions was enhanced in the beta band during the ON medication state. Therefore, our observations of the enhancement of such a coherent fronto-parietal motor network in the ON condition is consistent with this recent report. Such enhancement of FC is partially in agreement with another study which employed simultaneous fMRI/EEG recordings and showed that a higher dose of dopaminergic medication increased FC between motor areas and the default mode network in fMRI, whereas EEG connectivity remained unaffected (Evangelisti et al., 2019). In general, the dopaminergic effect over the cortico-cortical motor network might relate to the motor decision-making associated network, which has been shown to involve cortical fronto-parietal regions (Siegel et al., 2015), or it might relate to the default-mode network changes associated with non-motor symptoms in PD as suggested by other fMRI studies (Gao and Wu, 2016). Notably, a recent EEG study in PD using source localization demonstrated the presence of strong phase-amplitude coupling between the phase of beta and the amplitude of broadband gamma oscillations in a variety of cortical regions (including sensorimotor, somatosensory, and prefrontal areas) involved in motor and executive control (Gong et al., 2021). In line with this study, our findings of increased connectivity between centroparietal-frontal regions after dopaminergic medication further emphasize the importance of cortico-cortical connections in PD. These electrophysiological findings are consistent with previous fMRI studies suggesting a critical role of motor circuitry in PD in response to dopamine administration (Shen et al., 2020).

### Global and Local Network Organization

Using graph theory, we demonstrated that in the ON condition, there was a significant increase in node degree in centro-parietal

regions implying that these regions became more influential in the communication within the network. However, the network topology does not seem to undergo a major re-configuration as we did not identify significant changes in GE or CC in the brain network. This seems consistent with findings of previous studies in which PD patients were compared to healthy controls and no differences in topographical properties were found at the global level either in fMRI (Ruan et al., 2020) or in EEG in all frequency bands (Hassan et al., 2017). Another previous study also investigated the topographical structure of functional network using graph analysis based on MEG of patients with PD (Olde Dubbelink et al., 2013). Compared to healthy controls, their longitudinal study revealed a tendency toward a more random brain functional organization which was associated with lower local integration in multiple frequency bands and lower GE in the upper alpha band. However, another study using EEG found an increase in local integration and a decrease in GE across all the frequency bands in PD compared to healthy subjects (Utianski et al., 2016). In the present study, we explored the alterations in a functional spectral network using graph metrics and showed that dopaminergic medication intake did not significantly alter the brain network organization but did exert a significant enhancement in node degree of some particular regions within the network. The absence of significant changes in global integration and segregation of the functional network might suggest that dopaminergic medication does not re-configure the network at a global organizational level. Instead, these observations appear to imply that the brain network as a whole does not respond to medication at the complex (global integration and segregation) but rather at the low-level network topology (local node). It would be interesting for future studies to test whether this relates to the clinical improvement of symptoms and whether it is possible to significantly alter the network organization through different therapeutic interventions based on brain stimulation.

## Spectral Slope and Network Global Efficiency: Local E/I Balance and Global Network

A steeper spectral slope after dopaminergic medication intake was evident in PD. As proposed by previous computational work, the scaling property of the power spectrum of the membrane potentials and EEG could be due to the frequency attenuation of the extracellular medium itself (Bédard et al., 2006), or the intrinsic low-pass filtering effect of the electrical properties of the neural dendrites (Lindén et al., 2010; Einevoll et al., 2013). Alternatively, steepening of the slope could be a consequence of dampened activity propagation (Freeman and Zhai, 2009). More recently, by applying a realistic computational model, it has been demonstrated that stronger inhibitory activity results in steeper spectral decay compared to a situation with a stronger excitatory drive and thus the spectral slope value can be linked to the local excitation/inhibition ratio (Gao et al., 2017). Importantly, this spectral slope derived from ECoG recording dynamically reflects the effects of anesthesia induced by propofol. Furthermore, other pharmacological studies on resting state EEG confirmed further

that spectral slope can differentiate the states of wakefulness compared to a reduction or a complete loss of consciousness induced in the anesthesia (Colombo et al., 2019). Even though an exact generative mechanism of the 1/f shaped arrhythmic brain activity is still unclear (He, 2014), these recent prior work from simulations and experiments with the recordings across different spatial scales have indicated that the spectral slope could be a sensitive marker of the E/I dynamics. Following the E/I balance hypothesis of the spectral slope, a steeper slope after medication, observed in this study, may indicate that dopamine induced a state characterized by stronger inhibition over excitation. This line of interpretation agrees with previous TMS studies reporting a reduction of intracortical inhibition at rest in PD OFF medication (Ridding et al., 1995; Hanajima et al., 1996; Cantello, 2002) and an enhancement of evoked inhibitory activity (reflected in late TMS-evoked activity and beta TMS-evoked oscillations) after dopaminergic medication intake (Casula et al., 2017).

In addition, we found a close relationship between broadband non-oscillatory background activity measured by the spectral slope and the beta-band GE of the functional network. Global network efficiency represents the ability of integration of activity of widely distributed regions within a network, impacting information transmission and communication (Bullmore and Sporns, 2012). Notably, a previous simulation work demonstrated that synaptic E/I balance is crucial for efficient neural coding (Zhou and Yu, 2018), and the local E/I ratio plays a role in information transmission at large scale brain level (Deco et al., 2014). This theory concurs with our findings: the local and global spectral slope, reflecting the local and global tune of E/I balance, is closely associated with the functional network global integration property. The negative relationship between them implies that more excitation over inhibition corresponds to a lower level of functional network integration. Consistently, a recent study from both fMRI recording and simulation data showed that the local E/I ratio could have a significant impact on the organization of whole brain functional networks: GE of the functional network is an inverted-U shaped function of local E/I ratio and the more deviation from the balanced E/I state (in either direction), the lower GE of the whole functional network (Zhou et al., 2021). Our observation about the relationship between local and global slopes with the global network integration property can potentially be explained by this model: in OFF medication, an imbalanced E/I state (indexed by flatter slope) deviating from balanced E/I ratio exerts a monotonous negative relation with functional network GE. A presence of a negative relation between the spectral slope and GE might indicate that the network in PD OFF state resides within the left part of the inverted-U shaped function [GE vs. E/I ratio, refer to the Figure 8A of the study (Zhou et al., 2021)] where a monotonous correlation can be expected. Such a close association did not hold for the medication ON group. We assume that the medication moves the network back closer to a more balanced state, reflected in a steeper spectral slope (steepening of the flattened slope in OFF state); thus, functional network organization was no longer closely related to the E/I, since in a close-to balanced E/I state the GE would rather remain

stable (i.e., it reaches a maximum at the optimal E/I state). Our data did not show a difference in the network's GE property and in contrast did demonstrate a difference in E/I dynamics (reflected by the spectral slope) between the two conditions, thus actually providing a possibility which allows us to more specifically identify a position of the network in the OFF state. One intriguing explanation would be that GE changes rather slowly for quickly changing E/I ratio; therefore, the network in OFF condition stays relatively close to the one in ON condition along the GE axis, and along the E/I axis the networks from two conditions stay further apart.

The spatial distribution of local slope and GE demonstrated a specific pattern where the slope from the centro-parietal regions showed strongest relations with the GE of the brain network. In line with previous fMRI studies demonstrating that the nodal property of the parietal cortex is closely associated with motor outcome and decreased with progressing disease stage (Hoehn and Yahr stage) in PD (Sang et al., 2015; Fang et al., 2017; Suo et al., 2017), we assume that centro-parietal regions play an important role in orchestrating the whole global network organization. This is congruent with the finding that the connectivity patterns in these cortical regions are also affected by dopaminergic medication, as discussed above.

## LIMITATIONS

The first limitation of this study is that due to a rather low density of electrodes, we performed all connectivity analysis in sensor space. Thus, we refrain from making any conclusions about the specific structure of the networks (e.g., small-world and scale-free networks) as is also suggested in a critical study on the application of graph measures in EEG/MEG (Kaminski and Blinowska, 2018). It should also be noted that even if the analysis were to be conducted in source space, the volume conduction issue may still be present. Importantly, we applied a connectivity measure that is specifically used to overcome the volume conduction issue. Moreover, we were able to show that our findings remained consistent for a wide range of thresholds for the networks' properties.

Another limitation of our study is that clinical measures were not available and therefore, we could not associate EEG measures with the severity of clinical symptoms. We acknowledge this and suggest that future studies could include such a design so that the link between EEG parameters and clinical phenotypes can be explored. Future work should test whether and how local and global EEG parameters relate to clinical symptoms.

Lastly, due to the lack of EEG comparison with the healthy control group and the possibility to link the observed effects to differential components of the clinical symptoms in PD, we are rather restricted in our interpretation of the neuronal effects due to dopaminergic modulation. In particular, significant modulation of the spectral slopes and connectivity in some specific regions might potentially indicate a successful improvement associated with particular motor aspects (for

instance bradykinesia), while non-significant changes might indicate the absence of such modulation for other motor components such as internal motor control as shown in a recent study (Michely et al., 2015). Alternatively, the absence of neuronal changes in some regions might imply a co-existence of possible non-dopaminergic alterations (for instance serotonergic dysfunction) that could also become present in the course of PD and are not modulated by dopaminergic medication (Politis and Niccolini, 2015).

## CONCLUSION

Using multi-channel resting EEG recordings in PD patients, we showed differential effects of dopaminergic medication on local non-oscillatory components and connectivity parameters. Both from the local-level and brain-network perspective, the centro-parietal area was identified as the region where significant alterations in non-oscillatory wideband activity, measured by spectral slope and node centrality within the spectral functional network in the beta band, occurred. However, the network's global topologies, namely global integration (measured by GE) and global segregation (measured by CC) remained unaffected by the dopaminergic medication. Furthermore, during the OFF state, a close association between the spectral slopes (local and global) and network global integration was observed. These findings align with the theory that local E/I balance impacts global network structure, which might in turn demonstrate a crucial role of local non-oscillatory dynamics in forming the functional global integration in PD.

## DATA AVAILABILITY STATEMENT

Publicly available datasets were analyzed in this study. This data can be found here: <https://openneuro.org/datasets/ds002778>.

## ETHICS STATEMENT

The studies involving human participants were reviewed and approved by the Institutional Review Board Protocol at the University of California, San Diego. The patients/participants provided their written informed consent to participate in this study.

## AUTHOR CONTRIBUTIONS

JZ: conceptualization, methodology, software, formal analysis, data curation, writing—original draft, writing—review and editing, visualization, and project administration. AV: writing—review and editing, and supervision. VN: conceptualization, methodology, writing—original draft, writing—review and editing, project administration, and supervision. All authors contributed to the article and approved the submitted version.

## FUNDING

This work was supported by Deutsche Forschungsgemeinschaft (German Research Foundation) (Project ID: 424778381 TRR 295).

## ACKNOWLEDGMENTS

We thank Tilman Stephani for valuable discussions on the manuscript.

## SUPPLEMENTARY MATERIAL

The Supplementary Material for this article can be found online at: <https://www.frontiersin.org/articles/10.3389/fnagi.2022.846017/full#supplementary-material>

**Supplementary Figure 1 |** Normalized PSDs and connectivity profiles in OFF and ON conditions. In the upper panel: in OFF state, blue lines show the PSD profiles and black lines show the connectivity (left for C3-Pz and right for Fz-Pz). In the lower panel: in ON state, blue lines show the PSD profiles and red lines show the connectivity (left for C3-Pz and right for Fz-Pz).

**Supplementary Figure 2 |** Spectral slope effect remains the same after taking care of the cutting borders. **(A)** Left panel: grand mean PSD plot in PD ON

## REFERENCES

- Bassett, D. S., and Bullmore, E. T. (2009). Human brain networks in health and disease. *Curr. Opin. Neurol.* 22, 340–347. doi: 10.1097/WCO.0b013e32832d93dd
- Bédard, C., Kröger, H., and Destexhe, A. (2006). Does the 1/f frequency scaling of brain signals reflect self-organized critical states? *Phys. Rev. Lett.* 97:118102. doi: 10.1103/PhysRevLett.97.118102
- Benjamini, Y., and Hochberg, Y. (1995). Controlling the false discovery rate: a practical and powerful approach to multiple testing. *J. R. Stat. Soc. Lond. B Methodol.* 57, 289–300.
- Berman, B. D., Smucny, J., Wylie, K. P., Shelton, E., Kronberg, E., Leehey, M., et al. (2016). Levodopa modulates small-world architecture of functional brain networks in Parkinson's disease. *Mov. Disord.* 31, 1676–1684. doi: 10.1002/mds.26713
- Boon, L. I., Geraedts, V. J., Hillebrand, A., Tannemaat, M. R., Contarino, M. F., Stam, C. J., et al. (2019). A systematic review of MEG-based studies in Parkinson's disease: the motor system and beyond. *Hum. Brain Mapping.* 40, 2827–2848. doi: 10.1002/hbm.24562
- Boon, L. I., Hillebrand, A., Olde Dubbelink, K. T. E., Stam, C. J., and Berendse, H. W. (2017). Changes in resting-state directed connectivity in cortico-subcortical networks correlate with cognitive function in Parkinson's disease. *Clin. Neurophysiol.* 128, 1319–1326. doi: 10.1016/j.clinph.2017.04.024
- Bosboom, J. L. W., Stoffers, D., Wolters, E. C., Stam, C. J., and Berendse, H. W. (2009). MEG resting state functional connectivity in Parkinson's disease related dementia. *J. Neural Trans.* 116, 193–202. doi: 10.1007/s00702-008-0132-6
- Braak, H., Del Tredici, K., Rüb, U., De Vos, R. A. I., Jansen Steur, E. N. H., and Braak, E. (2003). Staging of brain pathology related to sporadic Parkinson's disease. *Neurobiol. Aging* 24, 197–211. doi: 10.1016/S0197-4580(02)00065-9
- Brown, P. (2003). Oscillatory nature of human basal ganglia activity: relationship to the pathophysiology of parkinson's disease. *Mov. Disord.* 18, 357–363. doi: 10.1002/mds.10358
- Bullmore, E., and Sporns, O. (2009). Complex brain networks: graph theoretical analysis of structural and functional systems. *Nat. Rev. Neurosci.* 10, 186–198. doi: 10.1038/nrn2575
- Bullmore, E., and Sporns, O. (2012). The economy of brain network organization. *Nat. Rev. Neurosci.* 13, 336–349. doi: 10.1038/nrn3214
- Cantello, R. (2002). Applications of transcranial magnetic stimulation in movement disorders. *J. Clin. Neurophysiol.* 19, 272–293. doi: 10.1097/00004691-200208000-00003
- Casarotto, S., Turco, F., Comanducci, A., Perretti, A., Marotta, G., Pezzoli, G., et al. (2019). Excitability of the supplementary motor area in Parkinson's disease depends on subcortical damage. *Brain Stimul.* 12, 152–160. doi: 10.1016/j.brs.2018.10.011
- Casula, E. P., Stampanoni Bassi, M., Pellicciari, M. C., Ponzo, V., Veniero, D., Peppe, A., et al. (2017). Subthalamic stimulation and levodopa modulate cortical reactivity in Parkinson's patients. *Park. Relat. Disord.* 34, 31–37. doi: 10.1016/j.parkreldis.2016.10.009
- Cesnaite, E., Steinfath, P., Idaji, M. J., Stephani, T., Haufe, S., Sander, C., et al. (2021). Alterations in rhythmic and non-rhythmic resting-state EEG activity and their link to cognition in older age. *bioRxiv [Preprint]* 1–34. doi: 10.1101/2021.08.26.457768
- Chai, M. T., Amin, H. U., Izhar, L. I., Saad, M. N. M., Abdul Rahman, M., Malik, A. S., et al. (2019). Exploring EEG effective connectivity network in estimating influence of color on emotion and memory. *Front. Neuroinform.* 13:66. doi: 10.3389/fninf.2019.00066
- Colombo, M. A., Napolitani, M., Boly, M., Gosseries, O., Casarotto, S., Rosanova, M., et al. (2019). The spectral exponent of the resting EEG indexes the presence of consciousness during unresponsiveness induced by propofol, xenon, and ketamine. *NeuroImage* 189, 631–644. doi: 10.1016/j.neuroimage.2019.01.024
- De Hemptinne, C., Swann, N. C., Ostrem, J. L., Ryapolova-Webb, E. S., San Luciano, M., Galifianakis, N. B., et al. (2015). Therapeutic deep brain stimulation reduces cortical phase-amplitude coupling in Parkinson's disease. *Nat. Neurosci.* 18, 779–786. doi: 10.1038/nn.3997
- Deco, G., Ponce-Alvarez, A., Hagmann, P., Romani, G. L., Mantini, D., and Corbetta, M. (2014). How local excitation-inhibition ratio impacts the whole brain dynamics. *J. Neurosci.* 34, 7886–7898. doi: 10.1523/JNEUROSCI.5068-13.2014
- Delorme, A., and Makeig, S. (2004). EEGLAB: an open source toolbox for analysis of single-trial EEG dynamics including independent component analysis. *J. Neurosci. Methods* 134, 9–21. doi: 10.1016/j.jneumeth.2003.10.009

condition before and after respecting the cutting borders (original PSD estimation in magenta and PSD estimation with taking care of the cutting borders in light blue). Two lines almost completely overlap across all the frequencies. Right panel: histograms of the estimated spectral slope values across all the channels and all the subjects within PD ON group with original approach in magenta and new approach (considering the borders) in light blue. **(B)** Topographical pattern of the comparison of the spectral slope between two conditions based on the estimations considering the cutting borders (OFF vs. ON,  $p = 0.0240$ ). This topography is consistent with the **Figure 2C** of the main manuscript.

**Supplementary Figure 3 |** Functional connectivity effects remain unchanged after taking care of the borders introduced by removing the artifactual segments. **(A)** Left panel: averaged functional connectivity between Fz-Pz channels in PD OFF condition before and after considering the cutting borders (original and new estimation in magenta and light blue color, respectively). Two approaches give rise to very similar estimation values. Right panel: same analysis but in the PD ON condition. **(B)** Topographical pattern of the comparison of the Fz-seed based functional connectivity between two conditions (OFF vs. ON,  $p = 0.028$ ). The significant cluster is highlighted by the labels in white, while the seed channel Fz is marked in yellow outlined by a square box. This spatial difference pattern is very consistent with the lower panel of **Figure 4B** of the main manuscript.

**Supplementary Figure 4 |** Spatial patterns for the correlation between local slope and global efficiency (beta network and under a variety of thresholding values). Significant channels are shown in labels ( $p < 0.05$ ) after FDR correction. Color bar indicates the correlation coefficient value. The spatial specificity over the centro-parietal region is generally consistent across a family of thresholding values (36–18%). At the PT% of 14%, a significant negative relationship is still present. For the higher PT% values, no significant correlation remains after multiple testing correction.

- Donoghue, T., Haller, M., Peterson, E. J., Varma, P., Sebastian, P., Gao, R., et al. (2020). Parameterizing neural power spectra into periodic and aperiodic components. *Nat. Neurosci.* 23, 1655–1665. doi: 10.1038/s41593-020-00744-x
- Einevoll, G. T., Kayser, C., Logothetis, N. K., and Panzeri, S. (2013). Modelling and analysis of local field potentials for studying the function of cortical circuits. *Nat. Rev. Neurosci.* 14, 770–785. doi: 10.1038/nrn3599
- Evangelisti, S., Pittau, F., Testa, C., Rizzo, G., Gramegna, L. L., Ferri, L., et al. (2019). L-dopa modulation of brain connectivity in Parkinson's disease patients: a pilot EEG-fMRI study. *Front. Neurosci.* 13:611. doi: 10.3389/fnins.2019.00611
- Fang, J., Chen, H., Cao, Z., Jiang, Y., Ma, L., Ma, H., et al. (2017). Impaired brain network architecture in newly diagnosed Parkinson's disease based on graph theoretical analysis. *Neurosci. Lett.* 657, 151–158. doi: 10.1016/j.neulet.2017.08.002
- Freeman, W. J., and Zhai, J. (2009). Simulated power spectral density (PSD) of background electrocorticogram (ECoG). *Cogn. Neurodyn.* 3, 97–103. doi: 10.1007/s11571-008-9064-y
- Gao, L. L., and Wu, T. (2016). The study of brain functional connectivity in Parkinson's disease. *Transl. Neurodegener.* 5:18. doi: 10.1186/s40035-016-0066-0
- Gao, R., Peterson, E. J., and Voytek, B. (2017). Inferring synaptic excitation/inhibition balance from field potentials. *NeuroImage* 158, 70–78. doi: 10.1016/j.neuroimage.2017.06.078
- George, J. S., Strunk, J., Mak-Mccully, R., Houser, M., Poizner, H., and Aron, A. R. (2013). Dopaminergic therapy in Parkinson's disease decreases cortical beta band coherence in the resting state and increases cortical beta band power during executive control. *NeuroImage Clin.* 3, 261–270. doi: 10.1016/j.nicl.2013.07.013
- Gong, R., Wegscheider, M., Mühlberg, C., Gast, R., Fricke, C., Rumpf, J. J., et al. (2021). Spatiotemporal features of  $\beta$ - $\gamma$  phase-amplitude coupling in Parkinson's disease derived from scalp EEG. *Brain* 144, 487–503. doi: 10.1093/brain/awaa400
- Hanajima, R., Ugawa, Y., Terao, Y., Ogata, K., and Kanazawa, I. (1996). Ipsilateral cortico-cortical inhibition of the motor cortex in various neurological disorders. *J. Neurol. Sci.* 140, 109–116. doi: 10.1016/0022-510X(96)00100-1
- Hassan, M., Chaton, L., Benquet, P., Delval, A., Leroy, C., Plomhause, L., et al. (2017). Functional connectivity disruptions correlate with cognitive phenotypes in Parkinson's disease. *NeuroImage Clin.* 14, 591–591. doi: 10.1016/j.nicl.2017.03.002
- He, B. J. (2014). Scale-free brain activity: past, present, and future. *Trends Cogn. Sci.* 18, 480–487. doi: 10.1016/j.tics.2014.04.003
- He, B. J., Zempel, J. M., Snyder, A. Z., and Raichle, M. E. (2010). The temporal structures and functional significance of scale-free brain activity. *Neuron* 66, 353–369. doi: 10.1016/j.neuron.2010.04.020
- Heinrichs-Graham, E., Kurz, M. J., Becker, K. M., Santamaria, P. M., Gendelman, H. E., and Wilson, T. W. (2014). Hypersynchrony despite pathologically reduced beta oscillations in patients with Parkinson's disease: a pharmacomagnetoencephalography study. *J. Neurophysiol.* 112, 1739–1747. doi: 10.1152/jn.00383.2014
- Herz, D. M., Eickhoff, S. B., Løkkegaard, A., and Siebner, H. R. (2014). Functional neuroimaging of motor control in parkinson's disease: a meta-analysis. *Hum. Brain Mapp.* 35, 3227–3237. doi: 10.1002/hbm.22397
- Hindriks, R. (2021). Relation between the phase-lag index and lagged coherence for assessing interactions in EEG and MEG data. *Neuroimage Rep.* 1:100007. doi: 10.1016/j.ynrp.2021.100007
- Hirschmann, J., Özkurt, T. E., Butz, M., Homburger, M., Elben, S., Hartmann, C. J., et al. (2011). Distinct oscillatory STN-cortical loops revealed by simultaneous MEG and local field potential recordings in patients with Parkinson's disease. *NeuroImage* 55, 1159–1168. doi: 10.1016/j.neuroimage.2010.11.063
- Hirschmann, J., Özkurt, T. E., Butz, M., Homburger, M., Elben, S., Hartmann, C. J., et al. (2013). Differential modulation of STN-cortical and cortico-muscular coherence by movement and levodopa in Parkinson's disease. *NeuroImage* 68, 203–213. doi: 10.1016/j.neuroimage.2012.11.036
- Hou, Y., Wei, Q., Ou, R., Yang, J., Song, W., Gong, Q., et al. (2018). Impaired topographic organization in cognitively unimpaired drug-naïve patients with rigidity-dominant Parkinson's disease. *Park. Relat. Disord.* 56, 52–57. doi: 10.1016/j.parkreldis.2018.06.021
- Jackson, N., Cole, S. R., Voytek, B., and Swann, N. C. (2019). Characteristics of waveform shape in Parkinson's disease detected with scalp electroencephalography. *eNeuro* 6:ENEURO.0151-19.2019. doi: 10.1523/ENEURO.0151-19.2019
- Jech, R., Mueller, K., Schroeter, M. L., and Růžička, E. (2013). Levodopa increases functional connectivity in the cerebellum and brainstem in Parkinson's disease. *Brain* 136:e234. doi: 10.1093/brain/awt015
- Kaminski, M., and Blinowska, K. J. (2018). Is graph theoretical analysis a useful tool for quantification of connectivity obtained by means of EEG/MEG Techniques? *Front. Neural Circ.* 12:76. doi: 10.3389/fncir.2018.00076
- Kühn, A. A., Tsui, A., Aziz, T., Ray, N., Brücke, C., Kupsch, A., et al. (2009). Pathological synchronisation in the subthalamic nucleus of patients with Parkinson's disease relates to both bradykinesia and rigidity. *Exp. Neurol.* 215, 380–387. doi: 10.1016/j.expneurol.2008.11.008
- Lantz, G., Grave de Peralta, R., Spinelli, L., Seeck, M., and Michel, C. M. (2003). Epileptic source localization with high density EEG: how many electrodes are needed? *Clin. Neurophysiol.* 114, 63–69. doi: 10.1016/S1388-2457(02)00337-1
- Lindén, H., Pettersen, K. H., and Einevoll, G. T. (2010). Intrinsic dendritic filtering gives low-pass power spectra of local field potentials. *J. Comput. Neurosci.* 29, 423–444. doi: 10.1007/s10827-010-0245-4
- Litvak, V., Jha, A., Eusebio, A., Oostenveld, R., Foltyniec, T., Limousin, P., et al. (2011). Resting oscillatory cortico-subthalamic connectivity in patients with Parkinson's disease. *Brain* 134, 359–374. doi: 10.1093/brain/awq332
- Melgari, J. M., Curcio, G., Mastrolilli, F., Salomone, G., Trotta, L., Tombini, M., et al. (2014). Alpha and beta EEG power reflects L-dopa acute administration in parkinsonian patients. *Front. Aging Neurosci.* 6:302. doi: 10.3389/fnagi.2014.00302
- Michely, J., Volz, L. J., Barbe, M. T., Hoffstaedter, F., Viswanathan, S., Timmermann, L., et al. (2015). Dopaminergic modulation of motor network dynamics in Parkinson's disease. *Brain* 138, 664–678. doi: 10.1093/brain/awu381
- Miller, A. M., Miocinovic, S., Swann, N. C., Rajagopalan, S. S., Darevsky, D. M., Gilron, R., et al. (2019). Effect of levodopa on electroencephalographic biomarkers of the parkinsonian state. *J. Neurophysiol.* 122, 290–299. doi: 10.1152/jn.00141.2019
- Milz, P., Faber, P. L., Lehmann, D., Kochi, K., and Pascual-Marqui, R. D. (2014). sLORETA intracortical lagged coherence during breath counting in meditation-naïve participants. *Front. Hum. Neurosci.* 8:303. doi: 10.3389/fnhum.2014.00303
- Mitsis, G. D., Anastasiadou, M. N., Christodoulakis, M., Paphathanasiou, E. S., Papacostas, S. S., and Hadjipapas, A. (2020). Functional brain networks of patients with epilepsy exhibit pronounced multiscale periodicities, which correlate with seizure onset. *Hum. Brain Mapp.* 41, 2059–2076. doi: 10.1002/hbm.24930
- Molina, J. L., Voytek, B., Thomas, M. L., Joshi, Y. B., Bhakta, S. G., Talledo, J. A., et al. (2020). Memantine effects on electroencephalographic measures of putative excitatory/inhibitory balance in schizophrenia. *Biol. Psychiatry Cogn. Neurosci. Neuroimaging* 5, 562–568. doi: 10.1016/j.bpsc.2020.02.004
- Müller, E. J., and Robinson, P. A. (2018). Suppression of parkinsonian beta oscillations by deep brain stimulation: determination of effective protocols. *Front. Comput. Neurosci.* 12:98. doi: 10.3389/fncom.2018.00098
- Olanow, C. W., Stern, M. B., and Sethi, K. (2009). The scientific and clinical basis for the treatment of Parkinson disease. *Neurology* 72(21 SUPPL. 4), S1–S136. doi: 10.1212/WNL.0b013e3181a1d44c
- Olde Dubbelink, K. T. E., Hillebrand, A., Stoffers, D., Deijen, J. B., Twisk, J. W. R., Stam, C. J., et al. (2014). Disrupted brain network topology in Parkinson's disease: a longitudinal magnetoencephalography study. *Brain* 137, 197–207. doi: 10.1093/brain/awt316
- Olde Dubbelink, K. T. E., Stoffers, D., Deijen, J. B., Twisk, J. W. R., Stam, C. J., Hillebrand, A., et al. (2013). Resting-state functional connectivity as a marker of disease progression in Parkinson's disease: a longitudinal MEG study. *NeuroImage Clin.* 2, 612–619. doi: 10.1016/j.nicl.2013.04.003
- Oostenveld, R., Fries, P., Maris, E., and Schoffelen, J. M. (2011). FieldTrip: open source software for advanced analysis of MEG, EEG, and invasive electrophysiological data. *Comput. Intell. Neurosci.* 2011:156869. doi: 10.1155/2011/156869

- Pascual-Marqui, R. D. (2007). Instantaneous and lagged measurements of linear and nonlinear dependence between groups of multivariate time series: frequency decomposition. *arXiv [Preprint]*. arXiv:0711.1455.
- Pascual-Marqui, R. D., Lehmann, D., Koukkou, M., Kochi, K., Anderer, P., Saletu, B., et al. (2011). Assessing interactions in the brain with exact low-resolution electromagnetic tomography. *Philos. Trans. R. Soc. A Math. Phys. Eng. Sci.* 369, 3768–3784. doi: 10.1098/rsta.2011.0081
- Peterson, E. J., Rosen, B. Q., Campbell, A. M., Belger, A., and Voytek, B. (2017). 1/f neural noise is a better predictor of schizophrenia than neural oscillations. *bioRxiv [Preprint]* doi: 10.1101/113449
- Politis, M., and Niccolini, F. (2015). Serotonin in Parkinson's disease. *Behav. Brain Res.* 277, 136–145. doi: 10.1016/j.bbr.2014.07.037
- Pollok, B., Kamp, D., Butz, M., Wojtecki, L., Timmermann, L., Südmeyer, M., et al. (2013). Increased SMA-M1 coherence in Parkinson's disease – Pathophysiology or compensation? *Exp. Neurol.* 247, 178–181. doi: 10.1016/j.expneurol.2013.04.013
- Ridding, M. C., Rothwell, J. C., and Inzelberg, R. (1995). Changes in excitability of motor cortical circuitry in patients with parkinson's disease. *Ann. Neurol.* 37, 181–188. doi: 10.1002/ana.410370208
- Robertson, M. M., Furlong, S., Voytek, B., Donoghue, T., Boettiger, C. A., and Sheridan, M. A. (2019). EEG power spectral slope differs by ADHD status and stimulant medication exposure in early childhood. *J. Neurophysiol.* 122, 2427–2437. doi: 10.1152/jn.00388.2019
- Rockhill, A. P., Jackson, N., George, J., Aron, A., Swann, N. C., et al. (2020). *UC San Diego Resting State EEG Data from Patients with Parkinson's Disease. OpenNeuro. [Dataset]*. doi: 10.18112/openneuro.ds002778.v1.0.4
- Ruan, X., Li, Y., Li, E., Xie, F., Zhang, G., Luo, Z., et al. (2020). Impaired topographical organization of functional brain networks in Parkinson's disease patients with freezing of gait. *Front. Aging Neurosci.* 12:580564. doi: 10.3389/fnagi.2020.580564
- Rubinov, M., and Sporns, O. (2010). Complex network measures of brain connectivity: uses and interpretations. *NeuroImage* 52, 1059–1069. doi: 10.1016/j.neuroimage.2009.10.003
- Sang, L., Zhang, J., Wang, L., Zhang, J., Zhang, Y., Li, P., et al. (2015). Alteration of brain functional networks in early-stage Parkinson's disease: a resting-state fMRI study. *PLoS One* 10:e0141815. doi: 10.1371/journal.pone.0141815
- Schapira, A. H. V. (2005). Present and future drug treatment for Parkinson's disease. *Journal of Neurology, Neurosurgery and Psychiatry* 76, 1472–1478. doi: 10.1136/jnnp.2004.035980
- Schaworonkoff, N., and Voytek, B. (2021). Longitudinal changes in aperiodic and periodic activity in electrophysiological recordings in the first seven months of life. *Dev. Cogn. Neurosci.* 47:100895. doi: 10.1016/j.dcn.2020.10.0895
- Sharma, A., Vidaurre, D., Vesper, J., Schnitzler, A., and Florin, E. (2021). Differential dopaminergic modulation of spontaneous cortico-subthalamic activity in parkinson's disease. *eLife* 10:e66057. doi: 10.7554/eLife.66057
- Shen, Y., Hu, J., Chen, Y., Liu, W., Li, Y., Yan, L., et al. (2020). Levodopa changes functional connectivity patterns in subregions of the primary motor cortex in patients With Parkinson's Disease. *Front. Neurosci.* 14:647. doi: 10.3389/fnins.2020.00647
- Siegel, M., Buschman, T. J., and Miller, E. K. (2015). Cortical information flow during flexible sensorimotor decisions. *Science* 348, 1352–1355. doi: 10.1126/science.aab0551
- Silberstein, P., Pogoyan, A., Kühn, A. A., Hotton, G., Tisch, S., Kupsch, A., et al. (2005). Cortico-cortical coupling in Parkinson's disease and its modulation by therapy. *Brain* 128, 1277–1291. doi: 10.1093/brain/awh480
- Smith, R. J., Alipourjehdi, E., Garner, C., Maser, A. L., Shrey, D. W., and Lopour, B. A. (2021). Infant functional networks are modulated by state of consciousness and circadian rhythm. *Netw. Neurosci.* 5, 614–630. doi: 10.1162/netn\_a\_00194
- Stam, C. J., Jones, B. F., Nolte, G., Breakspear, M., and Scheltens, P. (2007). Small-world networks and functional connectivity in Alzheimer's disease. *Cereb. Cortex* 17, 92–99. doi: 10.1093/cercor/bhj127
- Stanzione, P., Marciani, M. G., Maschio, M., Bassetti, M. A., Spanedda, F., Pierantozzi, M., et al. (1996). Quantitative EEG changes in non-demented Parkinson's disease patients before and during L-dopa therapy. *Eur. J. Neurol.* 3, 354–362. doi: 10.1111/j.1468-1331.1996.tb00229.x
- Steiner, H., and Kitai, S. T. (2001). Unilateral striatal dopamine depletion: time-dependent effects on cortical function and behavioural correlates. *Eur. J. Neurosci.* 14, 1390–1404. doi: 10.1046/j.0953-816X.2001.01756.x
- Stoffers, D., Bosboom, J. L. W., Deijen, J. B., Wolters, E. C., Berendse, H. W., and Stam, C. J. (2007). Slowing of oscillatory brain activity is a stable characteristic of Parkinson's disease without dementia. *Brain* 130, 1847–1860. doi: 10.1093/brain/awm034
- Stoffers, D., Bosboom, J. L. W., Wolters, E. C., Stam, C. J., and Berendse, H. W. (2008). Dopaminergic modulation of cortico-cortical functional connectivity in Parkinson's disease: an MEG study. *Exp. Neurol.* 213, 191–195. doi: 10.1016/j.expneurol.2008.05.021
- Sun, S., Li, X., Zhu, J., Wang, Y., La, R., Zhang, X., et al. (2019). Graph theory analysis of functional connectivity in major depression disorder with high-density resting state EEG Data. *IEEE Trans. Neural Syst. Rehabil. Eng.* 27, 429–439. doi: 10.1109/TNSRE.2019.2894423
- Suo, X., Lei, D., Li, N., Cheng, L., Chen, F., Wang, M., et al. (2017). Functional brain connectome and its relation to hoehn and yahr stage in Parkinson disease. *Radiology* 285, 904–913. doi: 10.1148/radiol.2017162929
- Swann, N. C., De Hemptinne, C., Aron, A. R., Ostrem, J. L., Knight, R. T., and Starr, P. A. (2015). Elevated synchrony in Parkinson disease detected with electroencephalography. *Ann. Neurol.* 78, 742–750. doi: 10.1002/ana.24507
- Tahmasian, M., Betray, L. M., van Eimeren, T., Drzezga, A., Timmermann, L., Eickhoff, C. R., et al. (2015). A systematic review on the applications of resting-state fMRI in Parkinson's disease: does dopamine replacement therapy play a role? *Cortex* 73, 80–105. doi: 10.1016/j.cortex.2015.08.005
- Tessitore, A., Cirillo, M., and De Micco, R. (2019). Functional connectivity signatures of Parkinson's disease. *Journal of Parkinson's Disease* 9, 637–652. doi: 10.3233/JPD-191592
- Tinkhauser, G., Pogoyan, A., Tan, H., Herz, D. M., Kühn, A. A., and Brown, P. (2017). Beta burst dynamics in Parkinson's disease off and on dopaminergic medication. *Brain* 140, 2968–2981. doi: 10.1093/brain/awx252
- Utianski, R. L., Caviness, J. N., van Straaten, E. C. W., Beach, T. G., Dugger, B. N., Shill, H. A., et al. (2016). Graph theory network function in parkinson's disease assessed with electroencephalography. *Clin. Neurophysiol.* 127, 2228–2236. doi: 10.1016/j.clinph.2016.02.017
- van den Heuvel, M. P., de Lange, S. C., Zalesky, A., Seguin, C., Yeo, B. T. T., and Schmidt, R. (2017). Proportional thresholding in resting-state fMRI functional connectivity networks and consequences for patient-control connectome studies: issues and recommendations. *NeuroImage* 152, 437–449. doi: 10.1016/j.neuroimage.2017.02.005
- van Wijk, B. C. M., Beudel, M., Jha, A., Oswal, A., Foltynie, T., Hariz, M. I., et al. (2016). Subthalamic nucleus phase-amplitude coupling correlates with motor impairment in Parkinson's disease. *Clin. Neurophysiol.* 127, 2010–2019. doi: 10.1016/j.clinph.2016.01.015
- Vecchio, F., Miraglia, F., Alù, F., Cotelli, M., Pellicciari, M. C., Judica, E., et al. (2021). Human brain networks in physiological and pathological aging: reproducibility of EEG graph theoretical analysis in cortical connectivity. *Brain Connect.* 12, 41–51. doi: 10.1089/brain.2020.0824
- Voytek, B., Kramer, M. A., Case, J., Lepage, K. Q., Tempesta, Z. R., Knight, R. T., et al. (2015). Age-related changes in 1/f neural electrophysiological noise. *J. Neurosci.* 35, 13257–13265. doi: 10.1523/JNEUROSCI.2332-14.2015
- Watts, D., and Strogatz, S. (1998). Collective dynamics of 'small-world' networks. *Nature* 393, 440–442. doi: 10.1038/30918
- Whitmer, D., de Solages, C., Hill, B., Yu, H., Henderson, J. M., and Bronte-Stewart, H. (2012). High frequency deep brain stimulation attenuates subthalamic and cortical rhythms in Parkinson's disease. *Fron. Hum. Neurosci.* 6:155. doi: 10.3389/fnhum.2012.00155
- Wingeier, B., Tchong, T., Koop, M. M., Hill, B. C., Heit, G., and Bronte-Stewart, H. M. (2006). Intra-operative STN DBS attenuates the prominent beta rhythm in the STN in Parkinson's disease. *Exp. Neurol.* 197, 244–251. doi: 10.1016/j.expneurol.2005.09.016
- Zeng, K., Wang, Y., Ouyang, G., Bian, Z., Wang, L., and Li, X. (2015). Complex network analysis of resting state EEG in amnesic mild cognitive impairment patients with type 2 diabetes. *Front. Comput. Neurosci.* 9:133. doi: 10.3389/fncom.2015.00133
- Zhang, J., Idaji, M. J., Villringer, A., and Nikulin, V. V. (2021). Neuronal biomarkers of Parkinson's disease are present in healthy aging. *NeuroImage* 243:118512. doi: 10.1016/j.neuroimage.2021.118512

- Zhou, S., and Yu, Y. (2018). Synaptic E-I balance underlies efficient neural coding. *Front. Neurosci.* 12:46. doi: 10.3389/fnins.2018.00046
- Zhou, X., Ma, N., Song, B., Wu, Z., Liu, G., Liu, L., et al. (2021). Optimal organization of functional connectivity networks for segregation and integration with large-scale critical dynamics in human brains. *Front. Comput. Neurosci.* 15:641335. doi: 10.3389/fncom.2021.641335

**Conflict of Interest:** The authors declare that the research was conducted in the absence of any commercial or financial relationships that could be construed as a potential conflict of interest.

**Publisher's Note:** All claims expressed in this article are solely those of the authors and do not necessarily represent those of their affiliated organizations, or those of the publisher, the editors and the reviewers. Any product that may be evaluated in this article, or claim that may be made by its manufacturer, is not guaranteed or endorsed by the publisher.

Copyright © 2022 Zhang, Villringer and Nikulin. This is an open-access article distributed under the terms of the Creative Commons Attribution License (CC BY). The use, distribution or reproduction in other forums is permitted, provided the original author(s) and the copyright owner(s) are credited and that the original publication in this journal is cited, in accordance with accepted academic practice. No use, distribution or reproduction is permitted which does not comply with these terms.